Supplementary Material

1 CONCEPT OF ANISOTROPY

Validation of the machine learning model in our case is a difficult process as we do not have ground-truth data available. As nanoporous gold is self-similar, we should see isotropy in all directions. We used two functions, namely the two-point correlation function and the lineal path function, to measure anisotropy in the microstructures. The two-point correlation function is the autocorrelation function showing the probability of finding another point of the same phase in the neighbourhood. Similarly, the lineal path function shows the probability of having two points in the same cluster. Both functions in all directions should remain very similar for the isotropic structures.

To test how well both functions work to detect anisotropy, we prepared one virtual structure with controlled anisotropy in the z-direction. This structure contained spheres stretched in the z-direction, making them elliptical in the +z direction. The intensity of the stretched part increases by going deeper in the z-direction to mimic the shine-through effect. Distances between each sphere layer in z-direction also change (Figure S1). These changes make the virtual structure isotropic in x and y-direction while anisotropic in the z-direction.

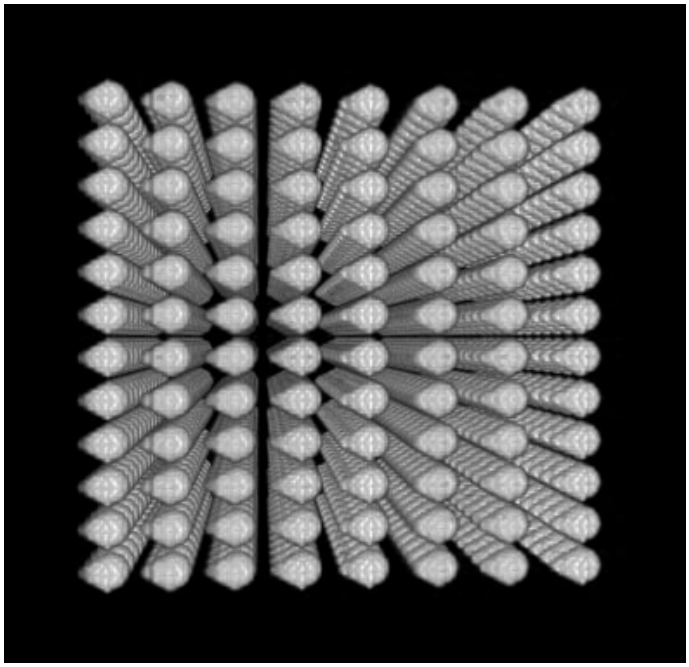

Figure S1. 3D view of virtual anisotropic structure

1.1 Test of isotropy – Two point correlation function

We calculated two-point correlation functions (Berryman, 1985) for prepared virtual structure in x, y and z-directions. As expected, we get the same two-point correlation functions in x and y-directions (yz and xz planes), but we get significantly different functions in the z-direction (xy plane) (Figure S2).

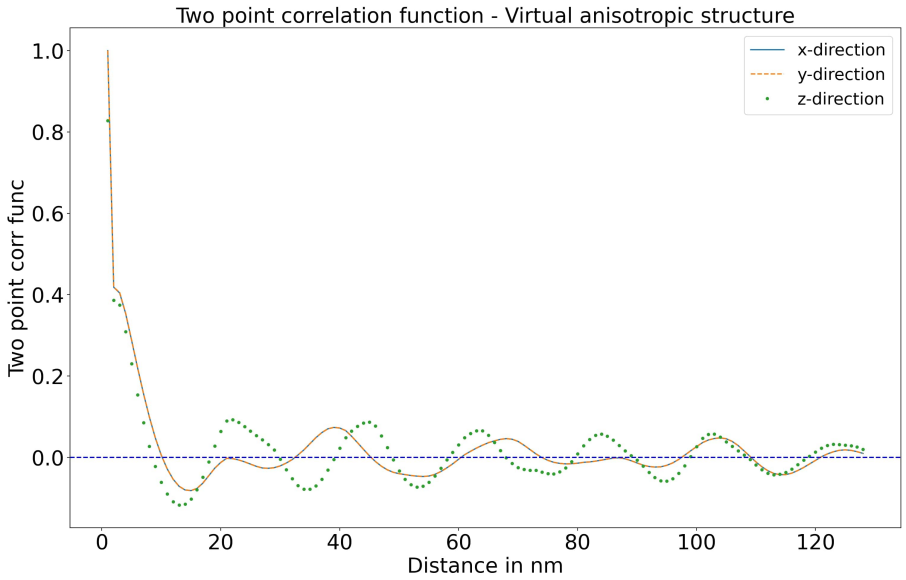

Figure S2. Two-point correlation function plots of virtual anisotropic structure in z-dir (xy plane), y-dir (xz plane) and x-dir (yz plane)

1.2 Test of isotropy – Lineal path function

(Torquato and Haslach Jr, 2002) proposed inserting lines of arbitrary length and orientation in the image and then counting the fraction of these lines that lie wholly within a single phase to calculate the Lineal path function. This function can also be useful to calculate average ligament size.

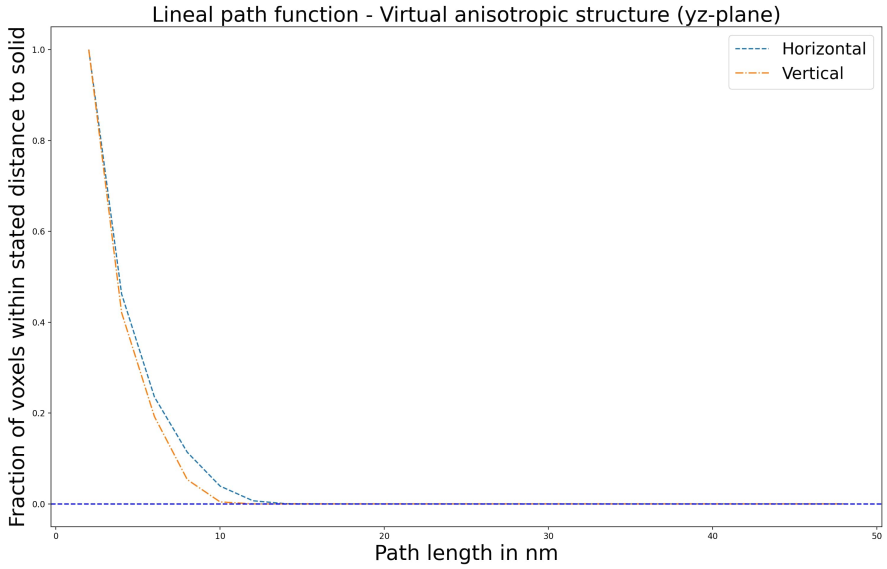

Figure S3. Lineal path function plots of virtual anisotropic structure in yz-plane

We have calculated a total of two lineal path functions whose directions are perpendicular to each other. Different lengths and errors between two functions suggest anisotropy in the structure. We repeated this procedure for all three planes.

As we know, there is some anisotropy in the z-direction; we can see length differences in the function in the yz-plane (Figure S3).

2 TRAINING PLOTS

In figures S4-S6, training/validation loss curves for different segmentation methods used in this research are shown. The figures show mean Dice loss over multiple epochs, with training scores (blue) and validation scores (orange). We used online data augmentation only during the training phase. Therefore, the training dataset was comparatively more complex than the validation dataset. Due to this complex training dataset, values of the Dice loss during the validation cycle are lower than values of the Dice loss during the training cycle in all three training/validation loss curves.

3 SUPPLEMENTARY TABLES AND FIGURES

REFERENCES

Berryman, J. G. (1985). Measurement of spatial correlation functions using image processing techniques. *Journal of Applied Physics* 57, 2374–2384

Torquato, S. and Haslach Jr, H. (2002). Random heterogeneous materials: microstructure and macroscopic properties. *Appl. Mech. Rev.* 55, B62–B63

3.1 Figures

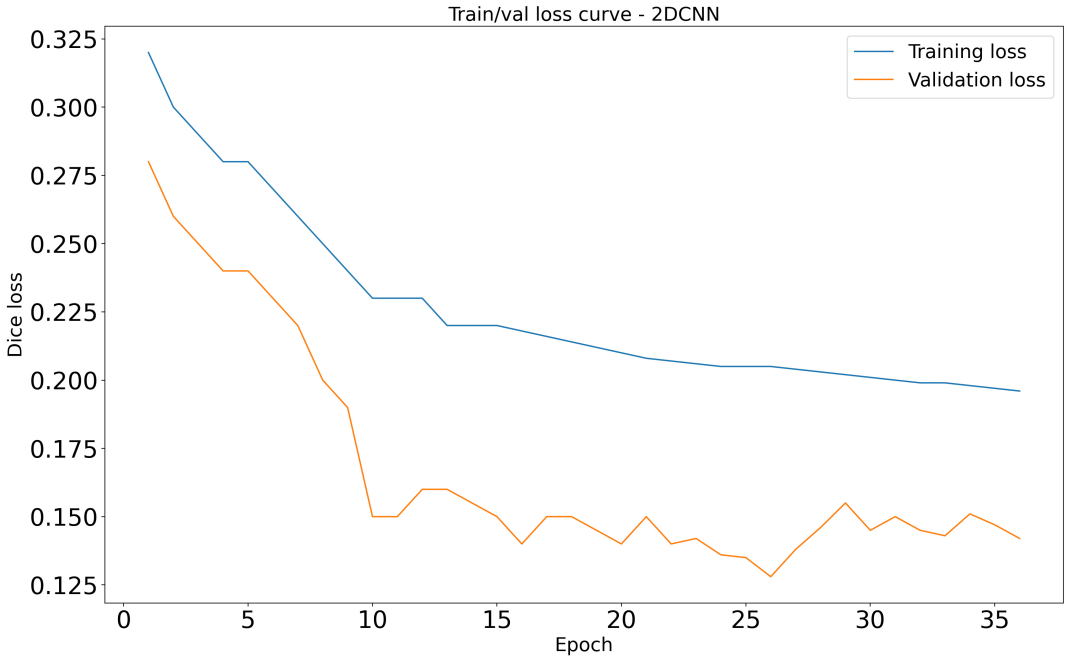

Figure S4. Training/validation loss curve for 2D CNN segmentation method

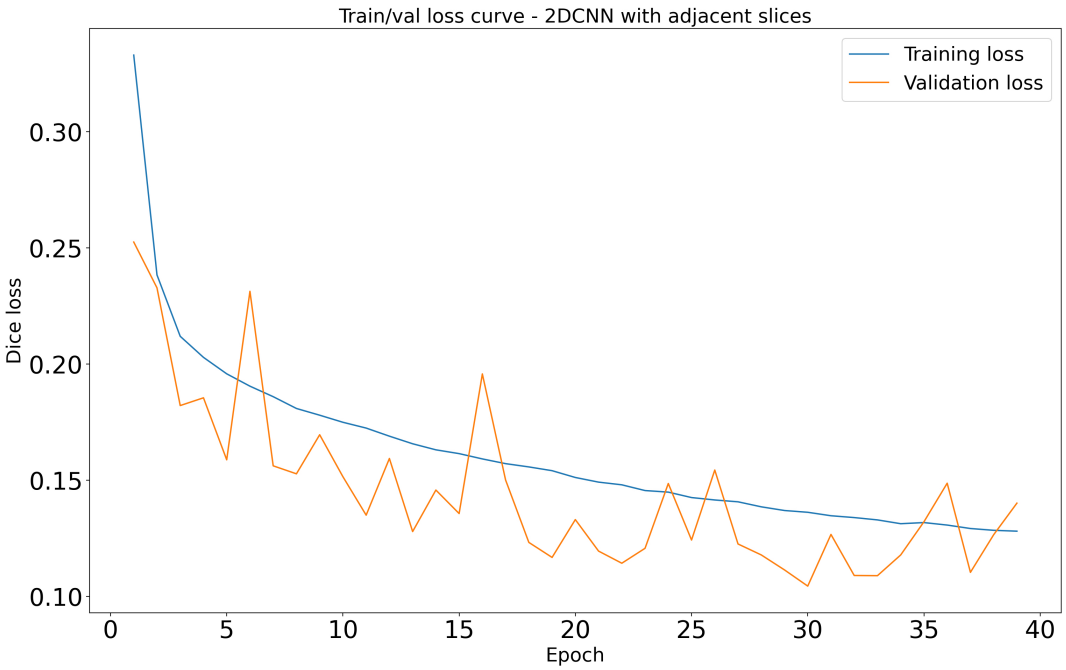

Figure S5. Training/validation loss curve for 2D CNN with adjacent slices segmentation method

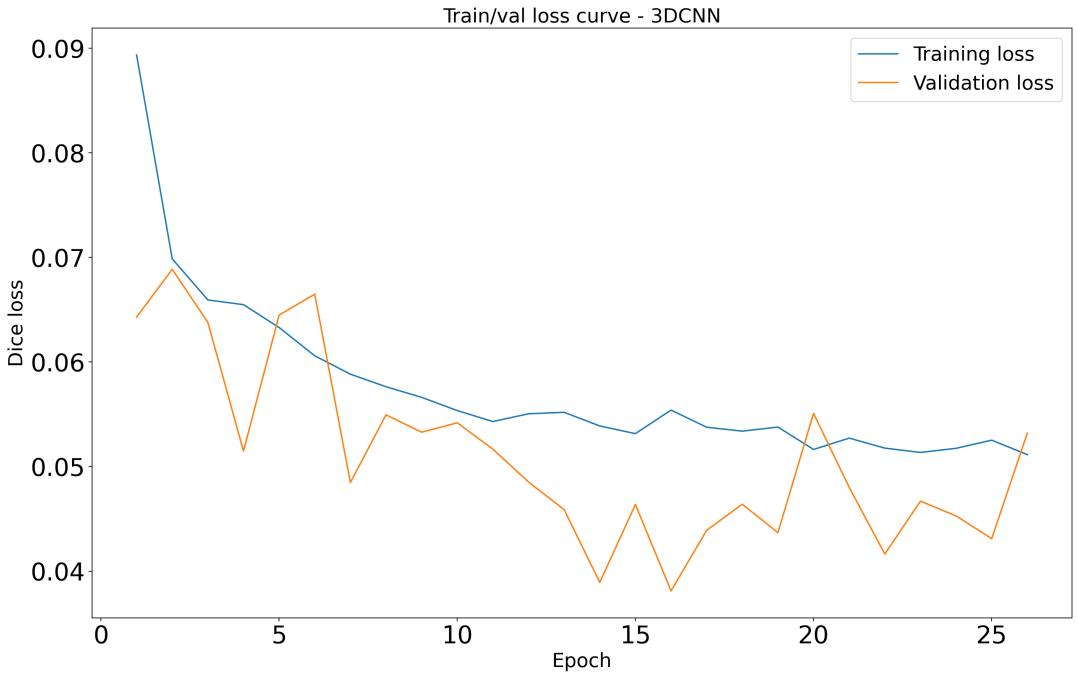

Figure S6. Training/validation loss curve for 3D CNN segmentation method

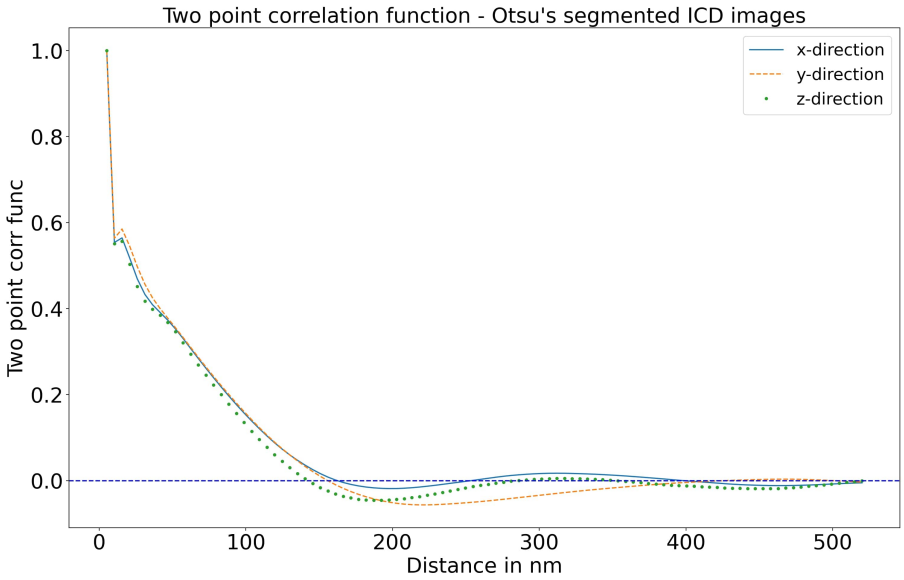

Figure S7. Two-point correlation function plots of segmented real hnpg_epoxy ICD dataset (using Otsu's method) in z-dir (xy plane), y-dir (xz plane) and x-dir (yz plane)

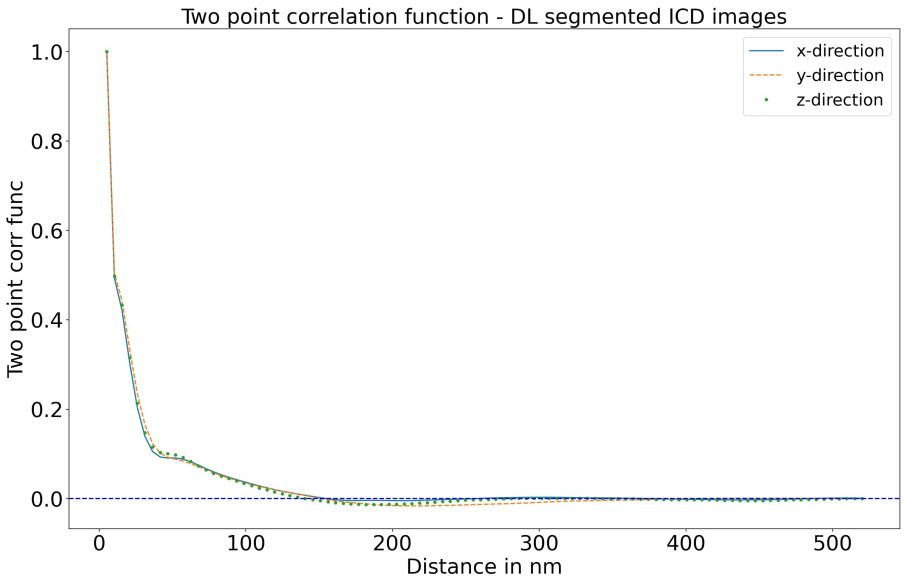

Figure S8. Two-point correlation function plots of segmented real hnpg_epoxy ICD dataset (using our deep learning method) in z-dir (xy plane), y-dir (xz plane) and x-dir (yz plane)

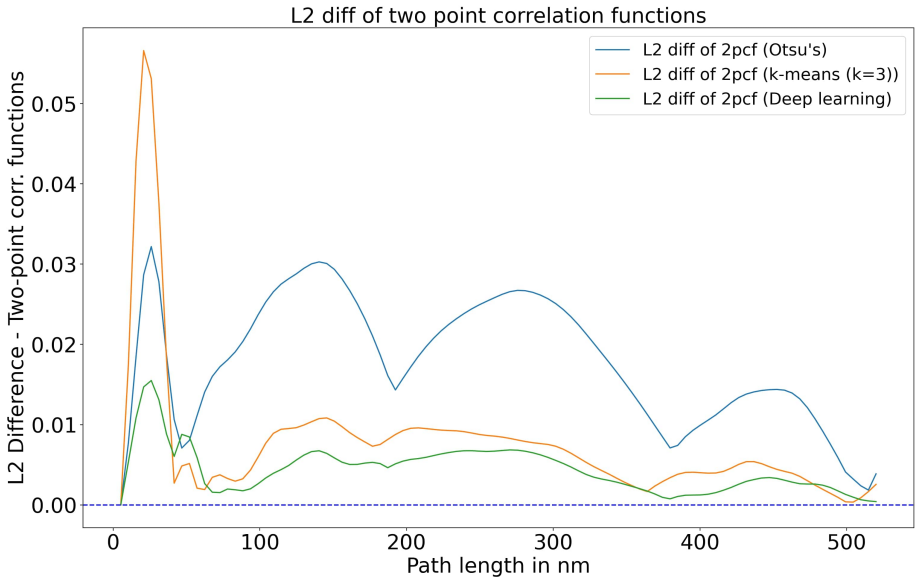

Figure S9. L2 differences of two-point correlation functions of segmented structures using Otsu's, k-means and our deep learning method

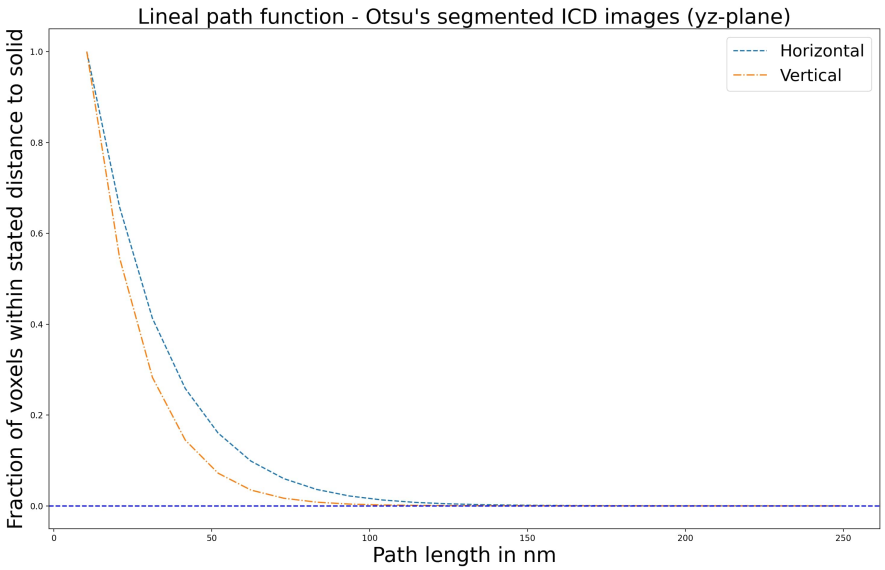

Figure S10. Lineal path function plots of segmented real hnpg_epoxy TLD dataset (using Otsu's method) in yz-plane

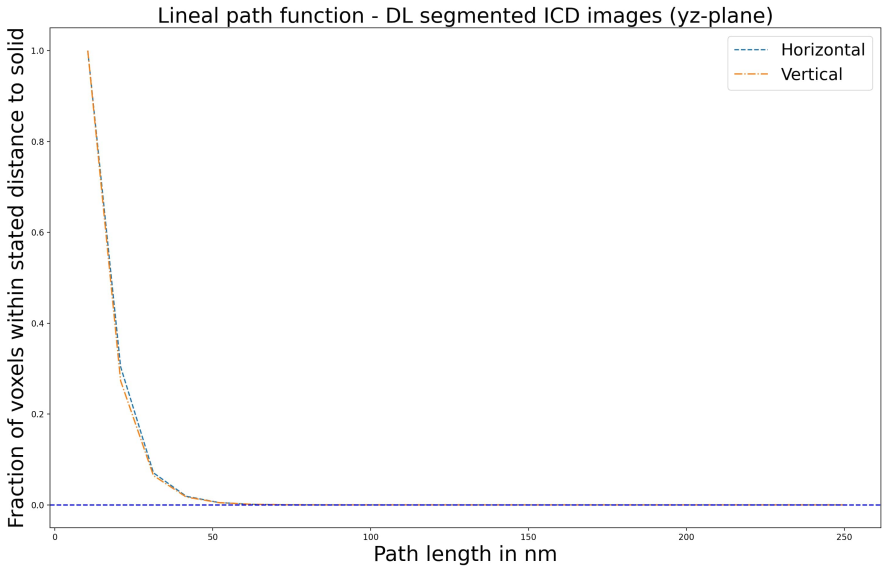

Figure S11. Lineal path function plots of segmented real hnpg_epoxy ICD dataset (using our deep learning method) in yz-plane

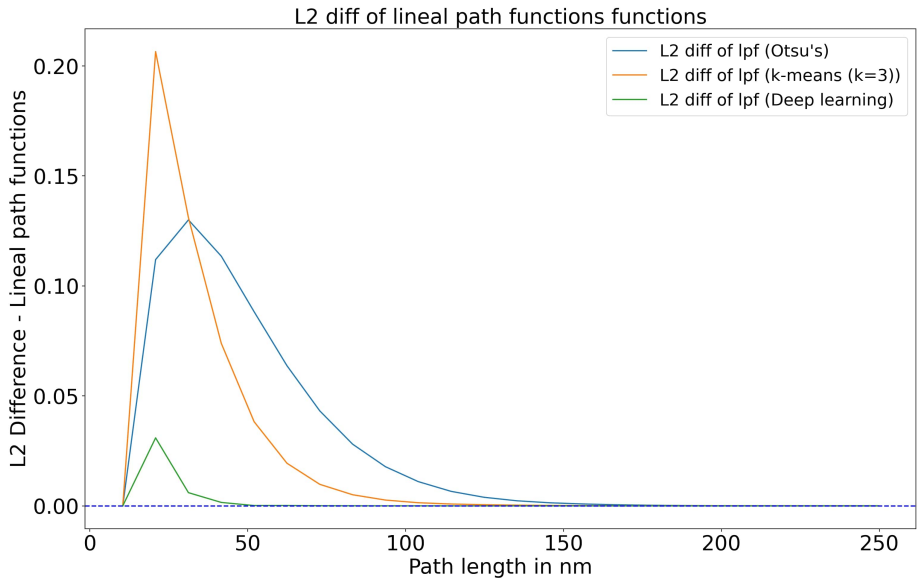

Figure S12. L2 differences of lineal path functions of segmented structures using Otsu's, k-means and our deep learning method

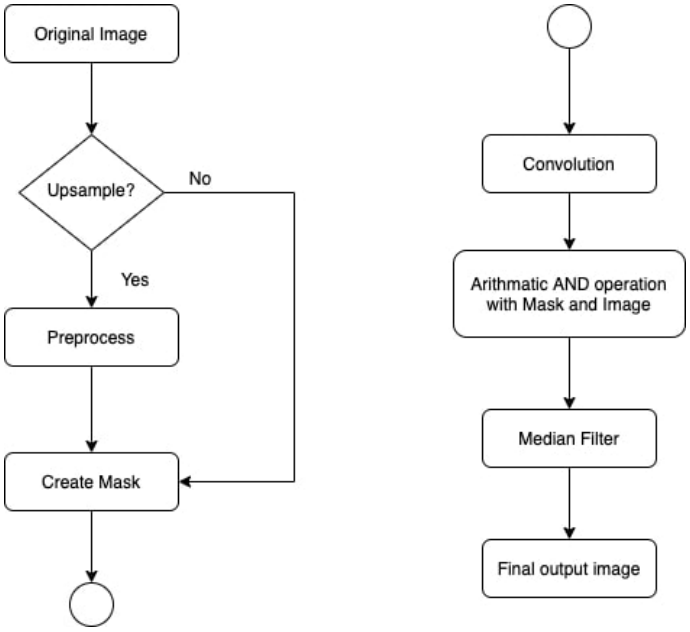

Figure S13. Methodology of SSM

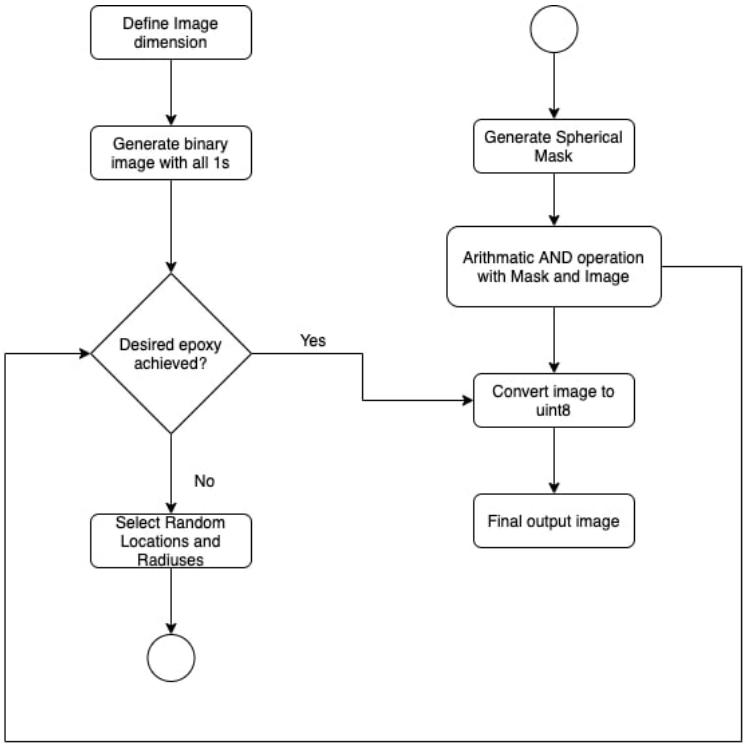

Figure S14. Methodology of RPGM